JACS
JOURNAL OF THE AMERICAN CHEMICAL SOCIETY
pubs.acs.org/JACS
Article

Regiospecific and Enantioselective Arylvinylcarbene Insertion of a C−H Bond of Aniline Derivatives Enabled by a Rh(I)-Diene Catalyst

Dong-Xing Zhu,[§] Hui Xia,[§] Jian-Guo Liu, Lung Wa Chung,* and Ming-Hua Xu*

Cite This: *J. Am. Chem. Soc.* 2021, 143, 2608−2619
Read Online
ACCESS | Metrics & More | Article Recommendations | Supporting Information

ABSTRACT: Asymmetric insertion of an arylvinylcarbenoid into the C−H bond for direct enantioselective C(sp^2)-H functionalization of aniline derivatives catalyzed by a rhodium(I)-diene complex was developed for the first time. The reaction occurred exclusively at the uncommon vinyl terminus site with excellent E selectivity and enantioselectivities, providing various chiral *γ,γ-gem*-diaryl-substituted *α,β*-unsaturated esters with broad functional group compatibility under simple and mild conditions. It provides a rare example of the asymmetric C−H insertion of arenes with selective vinylogous reactivity. Synthesis applications of this protocol were featured by several versatile product transformations. Systematic DFT calculations were also performed to elucidate the reaction mechanism and origin of the uncommon enantio- and regioselectivity of the Rh(I)-catalyzed C(sp^2)-H functionalization reaction. The measured and computed inverse deuterium kinetic isotope effect supports the C−C bond-formation step as the rate-determining step. Attractive interactions between the chiral ligand and substrates were also proposed to control the enantioselectivity.

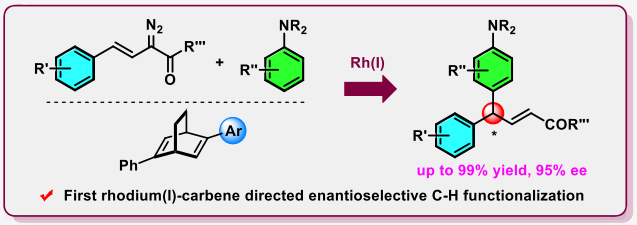

INTRODUCTION

Direct C−H functionalization is one of the most important and promising subjects in synthetic chemistry. Among them, transition-metal-catalyzed carbene or nitrene insertion represents an efficient and powerful approach to C−H functionalization.[1] Notably, the past decade has witnessed considerable developments of asymmetric C−H insertion with various metal-carbene precursors by different groups. In particular, a remarkable breakthrough in asymmetric C(sp^3)−H insertion has been made by the Davies group in recent years.[2] However, the achievement of asymmetric C(sp^2)−H insertion is not completely satisfactory. Despite some examples of asymmetric C−H insertion of electron-rich heteroarenes catalyzed by Rh(II)/Fe(II)/Pd(II)/Cu(I) carbene complexes,[3] such functionalization of less-reactive arenes by diazo compounds in an enantioselective manner has been underexplored. A notable exception is the Rh(II)-catalyzed enantioselective arylation of *α*-aryl-*α*-diazoacetates with aniline derivatives by using a chiral spiro phosphoric acid ligand as a cocatalyst reported by Zhou and Zhu in 2015.[4] Meanwhile, the Hu,[5] Zhou,[6a] and Zhang[6b,c] groups also realized the asymmetric C(sp^2)−H insertion of arenes independently by trapping zwitterionic intermediates generated from reactions of aryldiazoacetates and arenes with chiral electrophiles. Despite recent elegant progress, metal-carbene-mediated enantioselective direct intermolecular C-(sp^2)−H functionalization remains elusive and is largely limited to aryldiazoacetates.

Vinyldiazoacetates are unique and versatile carbene precursors because they form vinylcarbenoid intermediates upon treatment with transition metals.[7] In these metal-carbene complexes, electrophilic reactivity is intriguingly displayed at both the carbenoid and vinylogous positions (Scheme 1a). However, it is quite challenging to achieve sole addition at the vinyl terminus due to the intrinsically higher reactivity of the carbenoid site.[7c−e,8] Moreover, it could be difficult to achieve exclusive Z or E stereoselectivity as the reaction of substituted vinylcarbenoids is often accompanied by a Z/E configurational change in the C=C bond.[7c−e] In the seminal work by Davies,[9] vinylogous selectivity was formally achieved in the reaction with 1,2-dihydronaphthalenes and related cycloalkenes via a combined C−H functionalization/Cope rearrangement pathway in which the initial C−H functionalization step proceeds at the carbene site. Therefore, direct control of vinylogous reactivity as well as achieving both high Z/E selectivity and high enantioselectivity at the same time is synthetically challenging with substituted vinylcarbenoids,[8g,10] which has been underdeveloped. Despite many efforts in developing various transition-metal catalysts such as Mo,[7c] Ru(I),[7d] Ag(I),[7e,8d−g] Cu(I)/(II),[8a8g] and Rh(II)[8a−c] complexes to enhance vinylogous reactivity, challenging asymmetric variants of such chemistry for arylvinylcarbenoids remain unexplored (Scheme 1a).

Received: December 21, 2020
Published: February 4, 2021

https://dx.doi.org/10.1021/jacs.0c13191
J. Am. Chem. Soc. 2021, 143, 2608−2619

Scheme 1. General Characteristic of Arylvinylcarbenoids and the Current Challenges

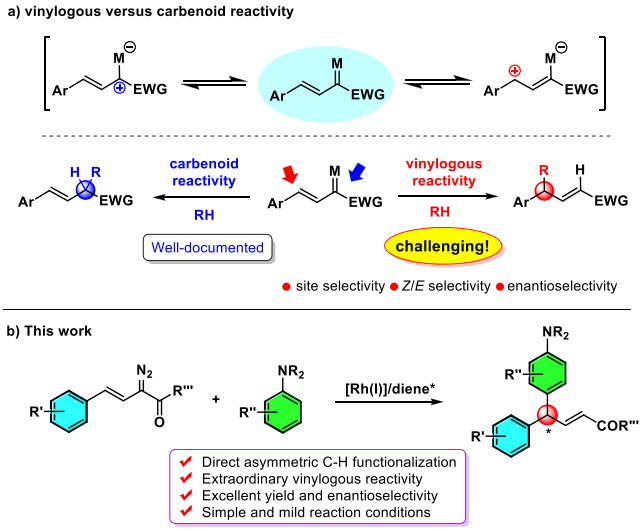

Recently, our laboratory has developed a series of C_1-symmetrical chiral dienes[11] based on Hayashi's biocyclo[2.2.2]octadiene framework and successfully employed them in Rh(I)-carbene-mediated asymmetric B−H and Si−H insertion.[12] On the basis of these studies and inspired by the great versatility of the Rh(I) carbenoid, we became interested in exploring the asymmetric C−H functionlization of aniline derivatives with arylvinyldiazoacetate through the Rh(I)-carbene strategy. Herein, we report a rhodium(I)-catalyzed regiospecific and direct enantioselective arylvinyldiazoacetate insertion of the C−H bond of aniline derivatives for the first time (Scheme 1b). This reaction occurred exclusively at the vinyl terminus site with sole E selectivity and high enantioselectivity to deliver chiral γ,γ-diaryl-α,β-unsaturated esters bearing a *gem*-diaryl carbon stereocenter.

RESULTS AND DISCUSSION

On the basis of our previous work,[12] we commenced our study by using $[Rh(C_2H_4)_2Cl]_2$ as the precatalyst (1.5 mol %) with C_1-symmetric chiral diene **L1** as the ligand (3.3 mol %) for the reaction of styryldiazoacetate **1** with 1-(3-methoxyphenyl)-pyrrolidine (**2a**). Pleasingly, the arylation reaction took place preferentially at the vinylogous site, and 2,6-dichlorophenyl styryldiazoacetate **1a** was found to be the most efficient substrate (details in the SI), providing corresponding product *E*-**3a** in 98% yield with promising enantioselectivity (91% ee, Table 1, entry 1). Unlike the previously reported Mo-, Ru(I)-, Ag(I)-, or Rh(II)-catalyzed vinylogous transformations with a mixture of E/Z products obtained,[7c−e] the Z isomer was not observed in this system. To further improve the enantioselectivity, a series of chiral diene ligands with different steric and electronic properties were examined (entries 2−9). However, no better results were obtained, except that **L8** exhibited the same performance (entry 8). A solvent screening revealed that chlorinated solvents were superior to the other solvents (entries 10−14). Changing CH_2Cl_2 to $CHCl_3$ resulted in a slightly improved enantioselectivity (93% ee), but the yield decreased to 84% (entry 11). To our delight, the yield can be improved to 96% when 5 mol % $MgBr_2{\cdot}Et_2O$ was added (entry 15). With the preprepared Rh(I)/diene (**L1**) complex, the reaction gave the best results (97% yield and 94% ee) (entry 16). Moreover, almost no product was observed in the absence of chiral diene ligands (entry 17). A byproduct (**4**) was also isolated in 13% yield, when $[Rh(COD)Cl]_2$ was used as a catalyst (entry 18). These experimental results suggest that our chiral diene ligand plays an essential role in the reaction. To understand whether other transition metals, which were commonly used to decompose diazo compounds, are also suitable catalysts for this reaction, we then examined the reaction with $Rh_2(OAc)_4$, AgOTf, and CuCl (entries 19−21). Interestingly, the use of $Rh_2(OAc)_4$ resulted in a very complicated reaction mixture with at least six different byproducts. AgOTf gave only a trace amount of the product. In the presence of CuCl, 30% yield of product was obtained. Therefore, in contrast to Rh(II), Ag(I), and Cu(I), the Rh(I)/diene catalyst was proved to be highly beneficial for the vinylogous C−C bond formation with high catalytic efficiency and excellent regio- and enantioselectivity.

With the optimized conditions in hand, we set out to investigate the scope of the vinyldiazo substrates (Scheme 2). Gratifyingly, various vinyldiazoacetates with different aromatic groups substituted at the vinyl terminus were all efficiently reacted with 1-(3-methoxyphenyl)pyrrolidine (**2a**) and gave the desired products in high yields (89−99%) with excellent enantioselectivities (90−95% ee). Generally, arylvinyldiazo-

Table 1. Optimization of Reaction Conditions

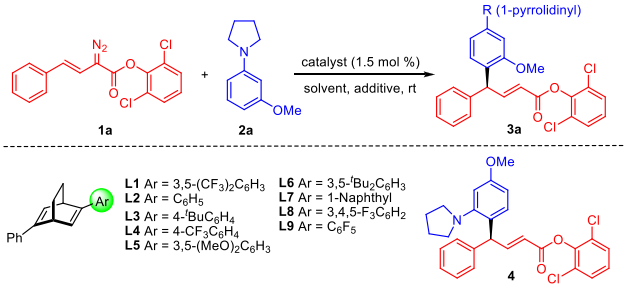

entry[a]	catalyst	solvent	yield (%)[b]	ee (%)[c]
1	$[Rh(C_2H_4)_2Cl]_2$, **L1**	DCM	98	91
2	$[Rh(C_2H_4)_2Cl]_2$, **L2**	DCM	39	85
3	$[Rh(C_2H_4)_2Cl]_2$, **L3**	DCM	35	81
4	$[Rh(C_2H_4)_2Cl]_2$, **L4**	DCM	89	89
5	$[Rh(C_2H_4)_2Cl]_2$, **L5**	DCM	22	78
6	$[Rh(C_2H_4)_2Cl]_2$, **L6**	DCM	39	85
7	$[Rh(C_2H_4)_2Cl]_2$, **L7**	DCM	16	79
8	$[Rh(C_2H_4)_2Cl]_2$, **L8**	DCM	98	91
9	$[Rh(C_2H_4)_2Cl]_2$, **L9**	DCM	48	82
10	$[Rh(C_2H_4)_2Cl]_2$, **L1**	DCE	97	91
11	$[Rh(C_2H_4)_2Cl]_2$, **L1**	$CHCl_3$	84	93
12	$[Rh(C_2H_4)_2Cl]_2$, **L1**	toluene	15	81
13	$[Rh(C_2H_4)_2Cl]_2$, **L1**	THF	16	90
14	$[Rh(C_2H_4)_2Cl]_2$, **L1**	Et_2O	24	81
15[d]	$[Rh(C_2H_4)_2Cl]_2$, **L1**	$CHCl_3$	96	93
16[d]	$[Rh(\mathbf{L1})Cl]_2$	$CHCl_3$	97	94
17	$[Rh(C_2H_4)_2Cl]_2$	$CHCl_3$		
18	$[Rh(COD)Cl]_2$	$CHCl_3$	65	
19	$Rh_2(OAc)_4$	$CHCl_3$	complex	
20	AgOTf	$CHCl_3$	trace	
21	CuCl	$CHCl_3$	30	

[a]Reactions were performed with **1a** (0.2 mmol) and **2a** (0.4 mmol) in the presence of 1.5 mol % $[Rh(C_2H_4)_2Cl]_2$ and 3.3 mol % ligand in solvent (4.0 mL) at rt for 6 h. [b]Isolated yield. [c]Determined by chiral HPLC. [d]$MgBr_2{\cdot}Et_2O$ (5 mol %) was added.

https://dx.doi.org/10.1021/jacs.0c13191
J. Am. Chem. Soc. 2021, 143, 2608−2619

Scheme 2. Scope of Arylvinyldiazoacetates[a,b,c]

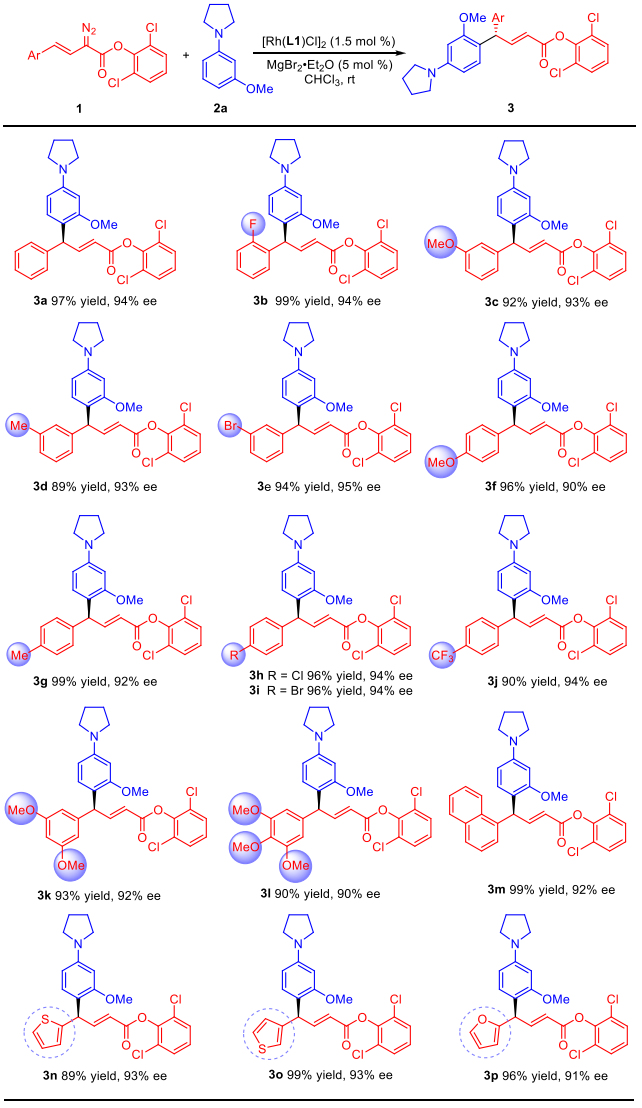

[a]Reactions were performed with **1** (0.2 mmol) and **2a** (0.4 mmol) in the presence of 1.5 mol % of $[Rh(L1)Cl]_2$, $MgBr_2{\cdot}Et_2O$ (5 mol %) in $CHCl_3$ (4.0 mL) for 6 h. [b]Isolated yield. [c]Determined by chiral HPLC.

acetates with electron-withdrawing substituents on the benzene ring gave slightly higher enantioselectivities than those with electron-donating substituents (**3b**, **3e**, **3h**, **3i**, and **3j** vs **3c**, **3d**, **3f**, **3g**, **3k**, and **3l**). It is noteworthy that aryl (Ar) could be a heteroaromatic substituent such as thienyl or furyl (**3n**, **3o**, or **3p**).

Next, the scope of aniline substrates was assessed under optimal conditions (Scheme 3). To our delight, 1-phenylpyrrolidine with a broad range of substituents (such as OMe, OEt, Me, Cl, OH, NHBoc, or CH_2OH) was applicable to the catalytic system, giving the corresponding products (**3q**−**3w**) in moderate to good yields with promising enantioselectivities (82−95% ee). In some cases, a slightly higher catalyst loading (2.5 mol %) was required to achieve better yields. Notably, upon using the less reactive chlorine-contained aniline, the reaction could also be performed, leading to desired product **3t** with good enantioselectivity (82% ee) albeit in a somewhat lower yield (42%). Most interestingly, both phenolic and

Scheme 3. Scope of Aniline Derivatives[a]

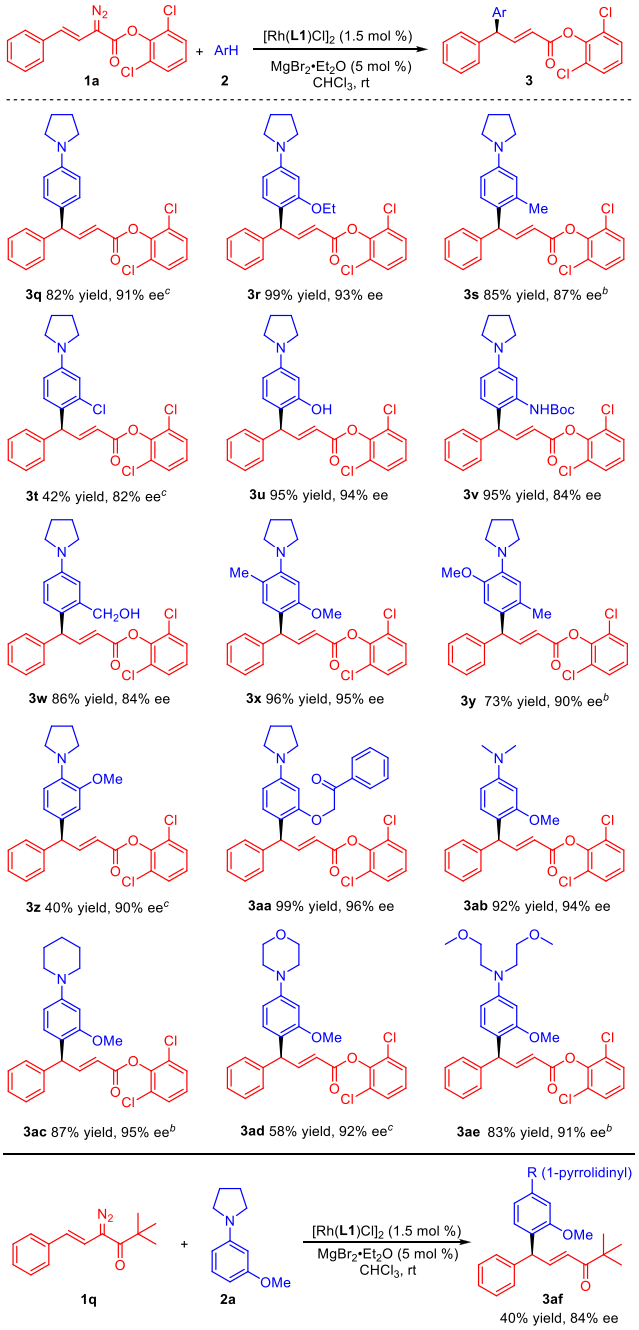

[a]Reactions were performed with **1** (0.2 mmol) and **2** (0.4 mmol) in the presence of 1.5 mol % $[Rh(L1)Cl]_2$ and $MgBr_2{\cdot}Et_2O$ (5 mol %) in $CHCl_3$ (4.0 mL) for 6 h; isolated product yields shown. [b]$[Rh(L1)Cl]_2$ (2.5 mol %) in $CHCl_3$. [c]$[Rh(L1)Cl]_2$ (2.5 mol %) in CH_2Cl_2.

benzylic hydroxyl groups are tolerated, and only C−H functionalization products **3u** and **3w** were formed in good yields under the reaction conditions, when 3-(pyrrolidin-1-yl)phenol and (3-(pyrrolidin-1-yl)phenyl)methanol were employed. No observation of the corresponding O−H insertion products demonstrates high chemoselectivity toward C−H insertion. To the best of our knowledge, achieving direct asymmetric C−H functionalization via a metal-carbene approach with a substrate bearing unprotected hydroxyl functionality has not been realized previously.[13] Moreover,

https://dx.doi.org/10.1021/jacs.0c13191
J. Am. Chem. Soc. 2021, 143, 2608−2619

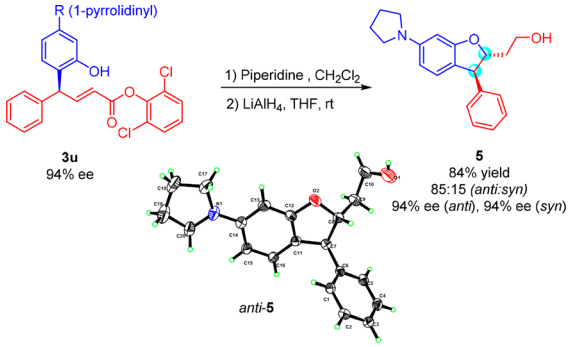

Figure 1. Derivation of **3u** and X-ray structure of *anti*-**5**.

Scheme 4. Transformation of Products

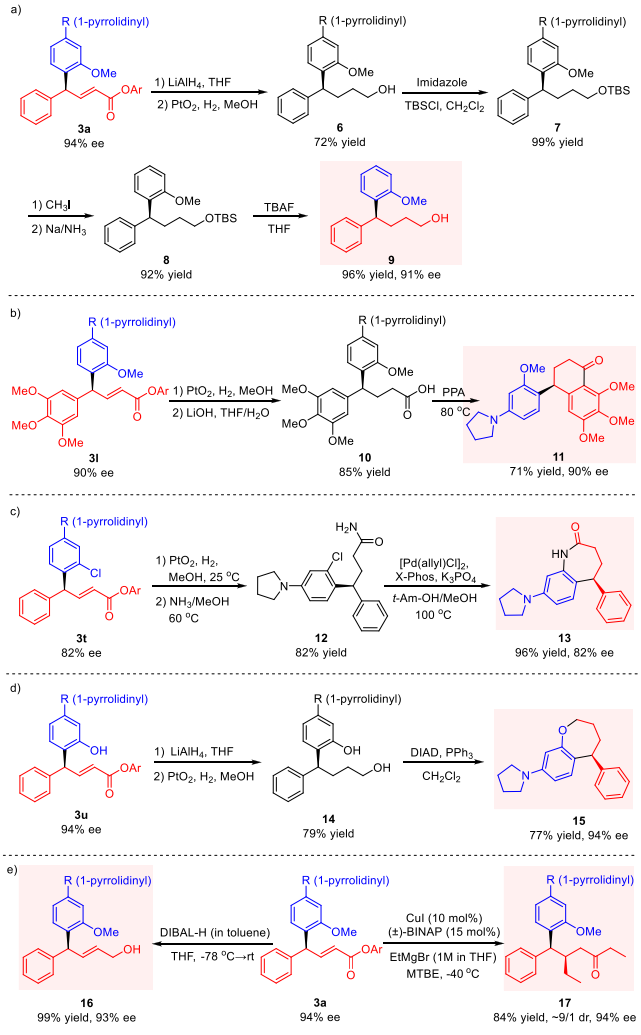

substrates **3x**–**3z** with substituents at ortho positions of the pyrrolidine ring and sterically congested substrate **3aa** are all well tolerated. Additionally, substituent effects on the aniline nitrogen were also evaluated. We were pleased to find that aniline derivatives bearing an *N*,*N*-dimethyl, piperidine, morpholine, or *N*,*N*-bis(2-methoxyethyl) structural moiety also underwent the desired C–H functionalization smoothly, delivering the corresponding products (**3ab**, **3ac**, **3ad**, and **3ae**) in high yields with essentially the same level of enantioselectivity (91–95% ee).

Scheme 5. Deuterium-Labeling Experiments

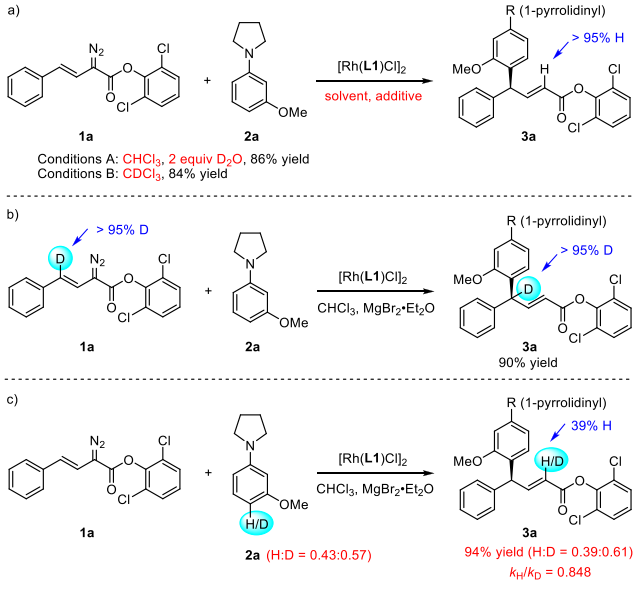

Scheme 6. Proposed Reaction Mechanism

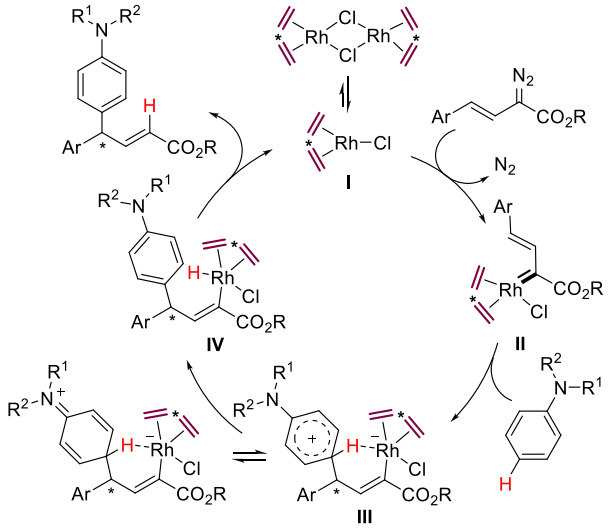

In addition to arylvinyldiazoacetates, we also attempted to extend the reaction to a more challenging arylvinyldiazoketone substrate. As noted by Davies,[14] arylvinyldiazoketone has rarely been used in transition-metal-catalyzed asymmetric X–H insertion reactions. We briefly examined the use of styryldiazoketone. To our satisfaction, styryldiazoketone was also found to be compatible with the current catalytic system, providing expected C–H functionalization product **3af** in 40% yield with 84% ee. The moderate yield of **3af** was associated with the instability of styryldiazoketone. This result further highlights the broad substrate scope of this direct asymmetric C–H functionalization protocol.

The absolute configuration of product **3u** was unambiguously determined by X-ray diffraction analysis of the single crystal of its *anti*-**5** derivative,[15] which was prepared from the oxa-Michael addition reaction of **3u** by taking advantage of the hydroxyl functionality at the ortho-aromatic carbon, followed by reduction with $LiAlH_4$ (Figure 1). It is worth mentioning that 2,3-dihydrobenzofurans are important heterocycles which

https://dx.doi.org/10.1021/jacs.0c13191
J. Am. Chem. Soc. 2021, 143, 2608–2619

Scheme 7. Calculated Relative Free Energies of Several Isomers of the Rh(I)-Vinylcarbenoid Intermediate in Solution by the SMD B3LYP-D3 Method

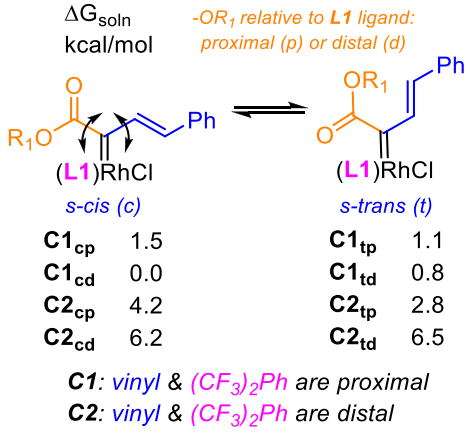

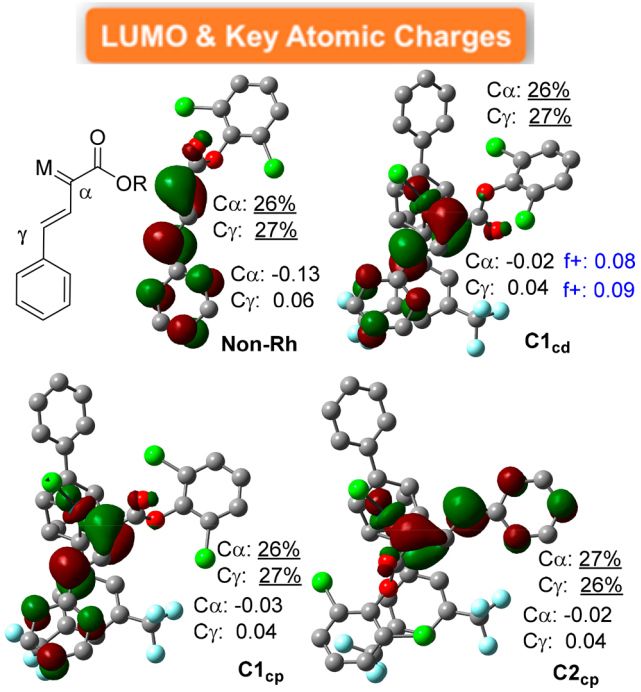

Figure 2. Calculated LUMO, Hirshfeld charge, and electrophilicity (f +, in blue color) for the two reacting carbon sites of the three key Rh(I)-vinylcarbenoid intermediates (**C1$_{cd}$**, **C1$_{cp}$**, and **C2$_{cp}$**) as well as the related carbene intermediate in the absence of the Rh(I)-ligand part (**Non-Rh**) in solution by the SMD B3LYP-D3 method.

are present in many biologically active compounds.[16] This procedure offers a convenient method for the construction of chiral 2,3-dihydrobenzofurans bearing two contiguous carbon stereocenters.

To further demonstrate the synthesis value of this method, a series of product transformations were conducted (Scheme 4). Compound **3a** was easily converted to alcohol **6** via successive reduction with $LiAlH_4$ and hydrogenation with PtO_2/H_2. Then, the hydroxyl of alcohol **6** was protected by using TBSCl. The deamination of product **7** with CH_3I and Na/NH_3, followed by deprotection of the TBS group of **8** under the TBAF conditions, provided *gem*-diaryl-substituted chiral butanol **9** in 88% yield with 91% ee over two steps. Notably, the chemoselective reduction of the C=C double bond of the *α,β*-unsaturated ester moiety could be readily achieved under the conditions of PtO_2/H_2. For example, **3l** was hydrogenated to give the desired product in 90% yield. Then, the ester hydrolysis with LiOH successfully afforded corresponding acid **10**, which was further converted to 3,4-dihydronaphthalen-1(2*H*)-one **11** through the intramolecular Friedel−Crafts reaction without eroding the enantioselectivity. In the other example, the hydrogenation of **3t** followed by aminolysis led to the formation of amide **12** in 82% overall yield. This amide was subsequently transformed to valuable benzo-fused lactam 1,3,4,5-tetrahydro-benzo[*b*]azepin-2-one **13** containing a chiral stereocenter in 96% yield with no ee erosion via an efficient palladium-catalyzed C−N coupling. We also explored the possibility of accessing benzo-fused oxygen-containing seven-membered-ring heterocycles. The subjection of **3u** to a tandem $LiAH_4$ and PtO_2/H_2 sequence, followed by the Mitsunobu reaction, furnished chiral 2,3,4,5-tetrahydrobenzo[*b*]oxepine **15** in good yield with the complete retention of enantiopurity. It is noteworthy that these derivation products bearing *gem*-diaryl chirality would be difficult to access using other synthesis strategies. In addition, the partial reduction of *α,β*-unsaturated esters to form the corresponding allylic alcohols (e.g., **16**) without a loss of enantioselectivity can be efficiently achieved with DIBAL-H. Moreover, *α,β*-unsaturated ester product **3a** was subjected to conjugate addition with Grignard reagent EtMgBr under the copper/BINAP catalyst system. Interestingly, this reaction proceeded cleanly and was found to produce 5-substituted 3-heptanone compound **17** as the only product (84% yield) with good diastereoselectivity (~9/1 dr) and excellent enantioselectivity (94% ee). The stereochemistry of the newly formed carbon center was determined by X-ray diffraction analysis of the single crystal of its derivative *N*-Ts hydrazone. (See the SI for details.) Thus, both intramolecular and intermolecular addition of the alkene moiety of the *α,β*-unsaturated ester products can be achieved.

Subsequently, the practicality of this catalytic method was evaluated by conducting the reaction of 2,6-dichlorophenyl styryldiazoacetate **1a** with 1-(3-methoxyphenyl)pyrrolidine **2a** on a 4.0 mmol scale (1.33 g) under the standard conditions. To our delight, this gram-scale reaction smoothly furnished desired insertion product **3a** in a comparable yield (95%) and with maintained enantioselectivity (93% ee). (See the SI for details.)

To gain some insight into the reaction mechanism, a combined experimental and computational study was then performed. A set of deuterium-labeling experiments were carried out. First, **3a** was obtained with no deuterium incorporated in the presence of D_2O or $CDCl_3$, indicating that the *α*-hydrogen does not come from solvent or residue water (Scheme 5a). To exclude the possible reaction pathway through a *π*-allyl-rhodium intermediate, deuterated phenyl-vinyldiazoacetate **1a** was prepared and subjected to the reaction conditions. Indeed, no migration of the deuterium atom to the *α*-carbon was observed (Scheme 5b). When 2 equiv of the aniline **2a**/**2a**-*d* (0.43:0.57) mixture was employed in the reaction, the product was obtained with 39% hydrogen at the *α*-position of the *α,β*-unsaturated ester (Scheme 5c). This result clearly indicates that the *α*-hydrogen atom is derived exclusively from the C4 position of aniline derivative. Furthermore, the proton transfer should not be the rate-determining step of the reaction because an inverse kinetic

https://dx.doi.org/10.1021/jacs.0c13191
J. Am. Chem. Soc. 2021, 143, 2608−2619

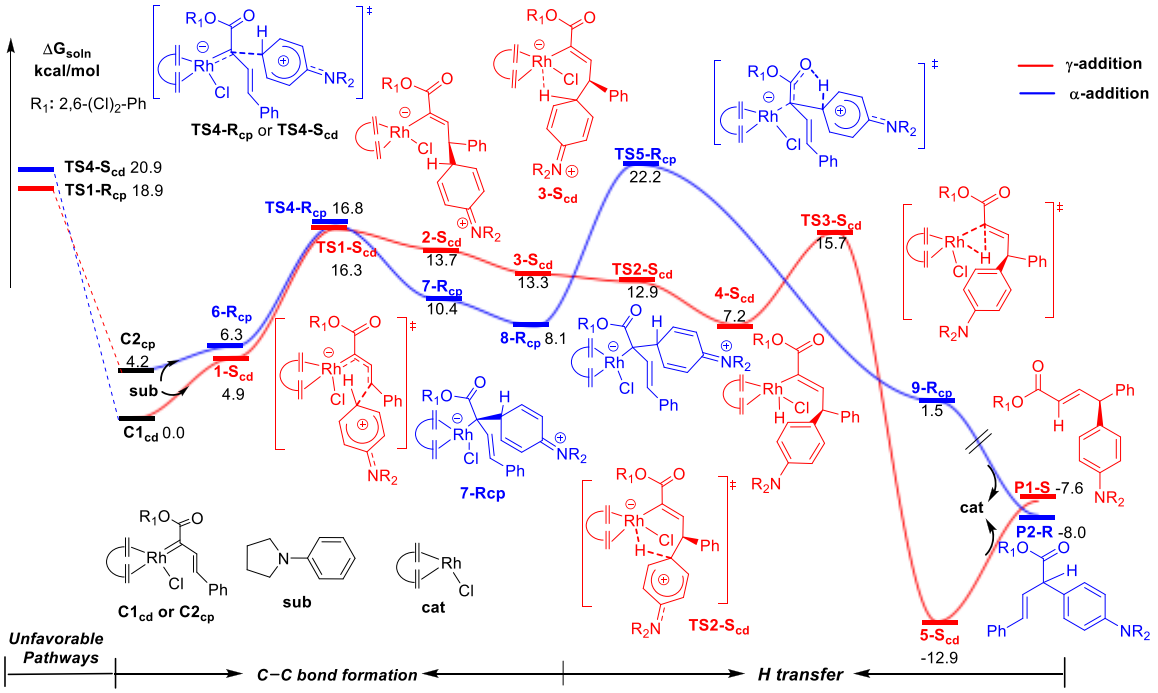

Figure 3. Calculated free-energy profiles for the most favorable γ-addition (**1**, **TS1**, **2**, **3**, **TS2**, **4**, **TS3**, and **5**) and α-addition (**6**, **TS4**, **7**, **8**, **TS5**, and **9**) pathways of the Rh(I)-catalyzed C−H functionalization of aniline in solution by the SMD B3LYP-D3 method. Their optimized 3D structures can be found in Figures S3 and S4. The pathways with the less favorable conformations are given in Figure S2 and Table S5. The detailed results for the transformation of **9-Rcp** to **P2-R** are given in Figure S8.

isotope effect ($k_H/k_D \approx 0.848$) was detected (*vide infra*) instead of the normal kinetic isotope effect (KIE).

On the basis of the above results, a plausible catalytic cycle is proposed in Scheme 6. Initially, active monorhodium catalyst **I** reacts with arylvinyldiazoacetate to generate an active Rh(I)-arylvinylcarbenoid species **II** in a *s-cis* configuration. The addition of the electron-rich phenyl ring of aniline onto carbene intermediate **II** at the vinyl terminus site forms zwitterionic intermediate **III**. Subsequently, **III** could undergo a 1,5-proton shift to form neutral Rh(III) intermediate **IV**, which after reductive elimination affords the desired product and regenerates catalytically active species **I**. Although the exact role of the $MgBr_2{\cdot}Et_2O$ additive in the yield increase is not clear, we proposed that the obtained α,β-unsaturated ester products may coordinate to active Rh-catalyst **I** after the last catalytic step and compete the sole coordination site with the new substrate for the subsequent catalytic cycles. Therefore, the addition of the $MgBr_2$ salt may facilitate the coordination with the insertion product to benefit the catalytic cycle.

A systematic DFT (SMD B3LYP-D3/6-31G*+SDD(Rh) method mainly) study was also carried out by using the chiral Rh(I)-diene catalyst, $[Rh(\mathbf{L1})Cl]_2$, as well as substrates **1a** and 1-phenylpyrrolidine.[7e,15,17] The relative stability of several possible isomers of the active Rh(I)-vinylcarbenoid intermediate (**II** in Scheme 6) was first examined (Scheme 7). As reported previously,[7e,17b] our DFT calculations generally show that the *s-cis* and *s-trans* conformations of the Rh(I)-vinylcarbenoid intermediate have comparable stability. In addition, *s-cis* intermediate $\mathbf{C1}_{cd}$ was computed to be the most stable conformation (Scheme 7). In this **C1**-type isomer, an aryl group of the arylvinylcarbenoid part is preferentially oriented to a closed quadrant of the catalyst to have $\pi-\pi$ stacking with the 3,5-$(CF_3)_2$Ph part of the **L1** ligand in $\mathbf{C1}_{cd}$, while the acetate part is positioned in an open quadrant (Figure 2).[18] $\mathbf{C1}_{cd}$ is lower in free energy than those with the opposite orientation of the arylvinylcarbenoid part by around 2.8−6.5 kcal/mol in solution (**C2**-type isomers, Scheme 7 and Figure 2). Interestingly, the two reacting vinylogous and carbenoid sites (i.e., Cγ and Cα) have the almost same contribution (26−27%) to LUMO in key *s-cis* intermediates $\mathbf{C1}_{cd}$, $\mathbf{C1}_{cp}$, and $\mathbf{C2}_{cp}$, which should interact with an occupied orbital of 1-phenylpyrrolidine for the new C−C bond construction with lower barriers (*vide infra*). Moreover, the computed Hirshfeld charge and electrophilicity (f+) on the Cγ and Cα sites are also similar. These computational results imply a similar reactivity on the Cγ and Cα sites for the initial C−C bond formation process (*vide infra*).

As shown in Figure 3, the most favorable pathway for forming the desired (*S*) γ,γ-diarylsubstituted α,β-unsaturated ester product (**P1-S**) is suggested to start with the coordination of 1-phenylpyrrolidine to $\mathbf{C1}_{cd}$ and form a weak $\mathbf{1\text{-}S}_{cd}$ complex (ΔG = 4.9 kcal/mol). It is followed by the C−C addition at the Cγ position via $\mathbf{TS1\text{-}S}_{cd}$ with a barrier of about 16.3 kcal/mol in solution to form zwitterionic intermediate $\mathbf{2\text{-}S}_{cd}$. $\mathbf{2\text{-}S}_{cd}$ undergoes $C_\beta-C\gamma$ bond rotation to give the $\mathbf{3\text{-}S}_{cd}$ isomer with the C−H → Rh agostic interaction.[19] Then, very facile proton transfer to the formal anionic Rh(I) metal from zwitterionic intermediate $\mathbf{3\text{-}S}_{cd}$ occurs to give a neutral Rh(III)-hydride vinyl intermediate $\mathbf{4\text{-}S}_{cd}$.[20] Finally, reductive elimination, which has a slightly lower barrier than the initial C−C formation step, affords the major (*S*)-product (**P1-S**) and regenerates active catalyst (**L1**)RhCl. To further prove the C−C formation step as the rate-determining step, secondary deuterium KIE on this step was computed using a deuterated 1-phenylpyrrolidine. A considerable inverse KIE (~0.81) for the 1-phenylpyrrolidine substrate, which mainly resulted from the change in hybridization on the Cγ site from C_{sp^2} to C_{sp^3},[21] was obtained by the SMD B3LYP-D3 method. The computed

https://dx.doi.org/10.1021/jacs.0c13191
J. Am. Chem. Soc. 2021, 143, 2608−2619

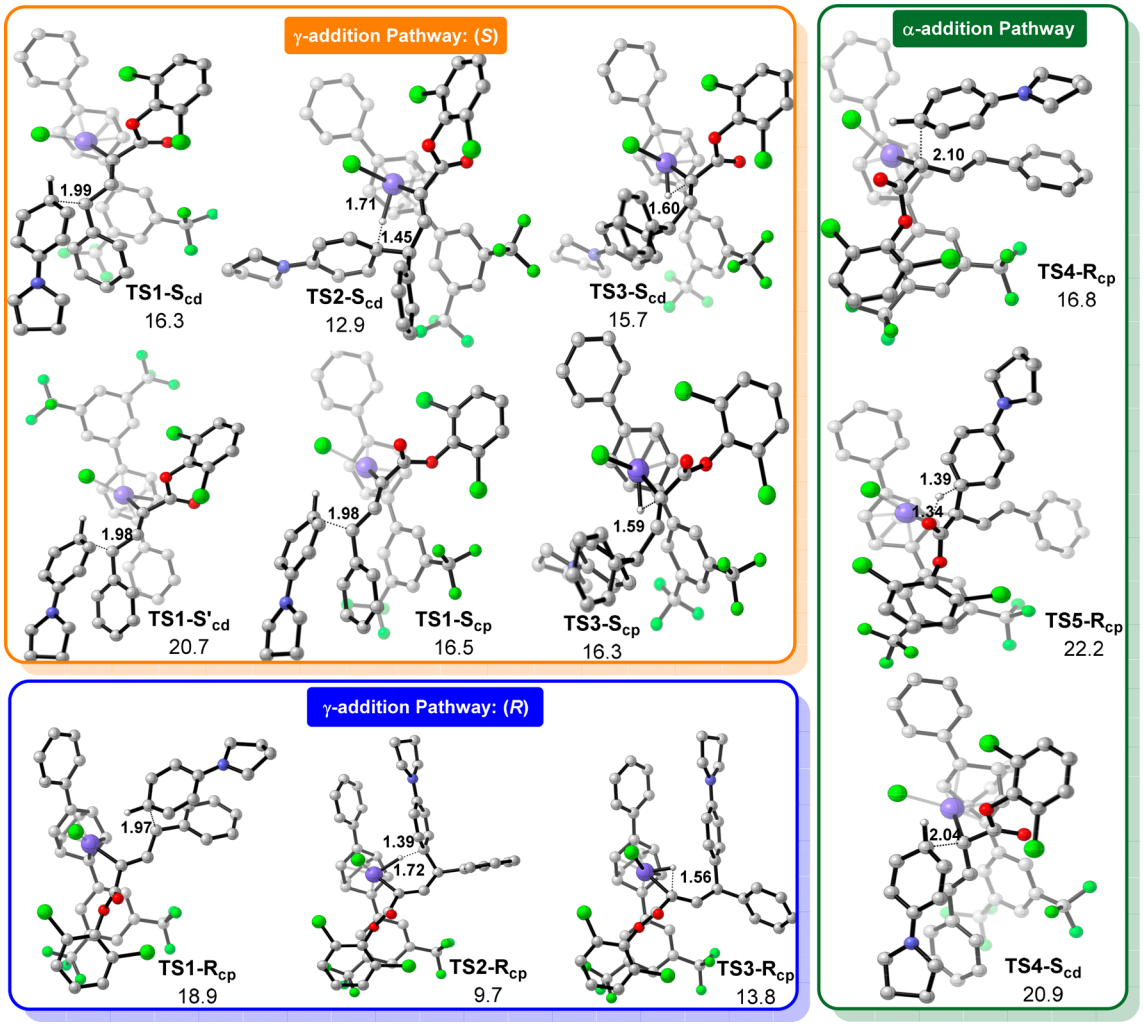

Figure 4. Optimized key transition-state structures of the regio- and stereoselective Rh(I)-catalyzed C−H functionalization with their relative free energy (in kcal/mol) and key distance (in Å) in solution by the SMD B3LYP-D3 method.

KIE value for the 1-phenylpyrrolidine substrate is qualitatively similar to the measured KIE value for the electron-rich and more reactive 1-(3-methoxyphenyl)pyrrolidine substrate (~0.848; Scheme 5c).[21d] Therefore, our combined experimental and computational results support the C−C formation step as the rate-determining step.

However, the corresponding addition at the Cα position from **C1**$_{cd}$ has to overcome a higher barrier (20.9 kcal/mol via **TS4-S**$_{cd}$, Figure 3). In comparison, the most favorable productive addition pathway at the Cα position also requires high barriers for the C−C formation step (16.8 kcal/mol via **TS4-R**$_{cp}$) and particularly for the subsequent proton transfer to the ester group via **TS5-R**$_{cp}$ (~22.2 kcal/mol above **C1**$_{cd}$).[19b] The latter process has to overcome a higher reaction barrier than the most favorable addition at the Cγ position via **TS1-S**$_{cd}$ by about 5.9 kcal/mol, which accounts for the observed regiospecific γ-addition.

Moreover, our DFT calculations show that, in the most favorable rate- and stereodetermining C−C addition step at the Cγ site, **TS1-S**$_{cd}$ (**C1**-type rearrangement) leading to the major enantiomeric (S)-product has a lower free-energy barrier than **TS1-R**$_{cp}$ (**C2**-type rearrangement), forming the minor (R)-product by 2.6 kcal/mol (Figures 4 and 5). Such a free-energy difference corresponds to the computed ee value of ~97.5%, which is close to the observed ee value of 91% (Scheme 3). The higher reaction barrier for the minor pathway can be attributed to the less stable resultant zwitterionic intermediate (ΔG = 17.7 and 13.7 kcal/mol for **2-R**$_{cp}$ and **2-S**$_{cd}$, respectively). Relative distortion/interaction analysis[22] was performed to further understand the stereoselectivity of the vital C−C formation step (Figure 6a). Unstable **C2**-type active species **C2**$_{cp}$ (ΔE = 3.1 kcal/mol) and a higher distortion energy ($\Delta\Delta E_{dist}$ = 2.8 kcal/mol, especially that on the metal-carbene and ligand part, 2.4 kcal/mol) play critical roles in determining the stereoselectivity. In this regard, noncovalent interaction (NCI) analysis[23] indicates the $\pi-\pi$ stacking between the aryl group of the arylvinylcarbenoid part and the 3,5-$(CF_3)_2$Ph part of the **L1** ligand as well as the dispersion of one chloro group of the ester with the C_6H_5 group of **L1** (pink circle in Figure 6b) in **TS1-S**$_{cd}$. The interactions should contribute some stabilization to **C1**$_{cd}$ (ΔG = 0.0 vs = 4.2 kcal/mol for **C2**$_{cp}$) and to their C−C bond formation step. In addition, owing to Hammond's postulate, a less stable zwitterionic intermediate **2-R**$_{cp}$ should be associated with a later transition state **TS1-R**$_{cp}$ (C−C: 1.97 Å vs 1.99 Å for **TS1-S**$_{cd}$; see Figure 4), which thus leads to a higher distortion energy.

https://dx.doi.org/10.1021/jacs.0c13191
J. Am. Chem. Soc. 2021, 143, 2608−2619

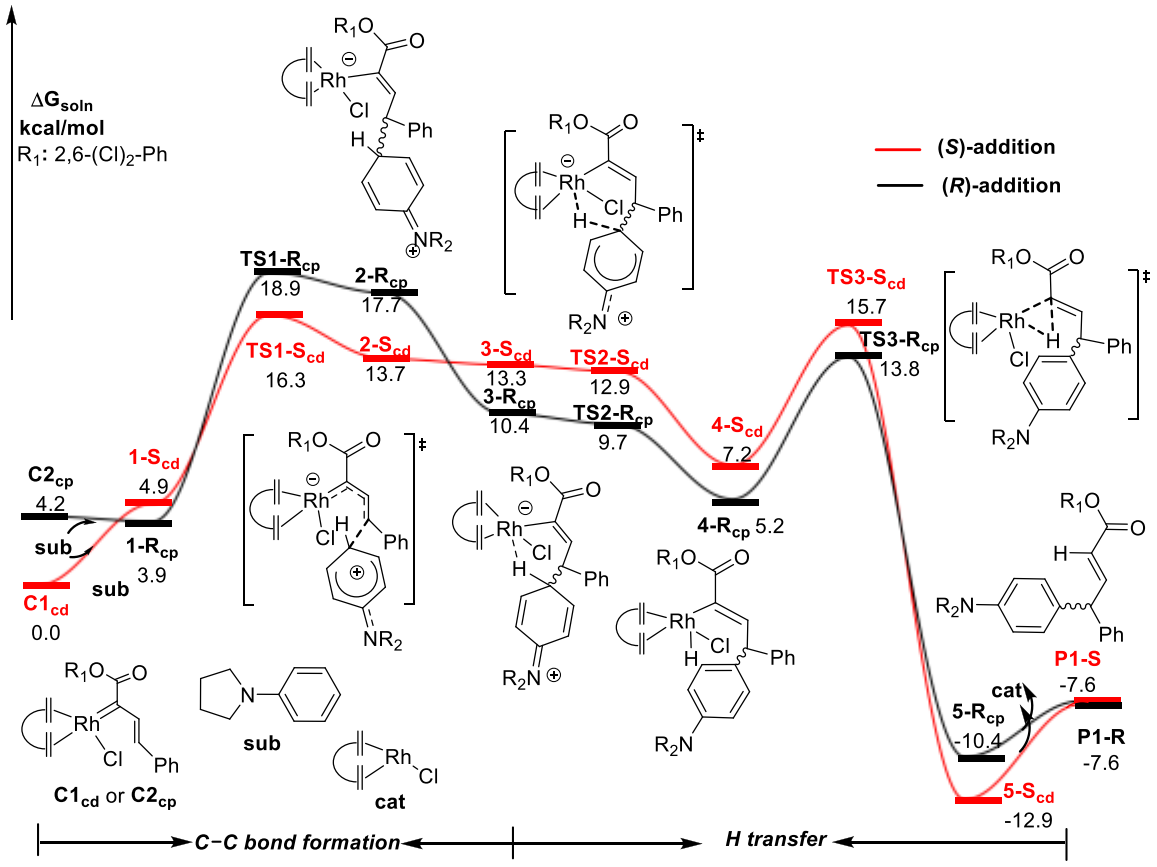

Figure 5. Calculated free-energy profiles for the key stereoselectivity of the Rh(I)-catalyzed C−H functionalization of aniline in solution by the SMD B3LYP-D3 method. Their optimized 3D structures can be found in Figures S3 and S5.

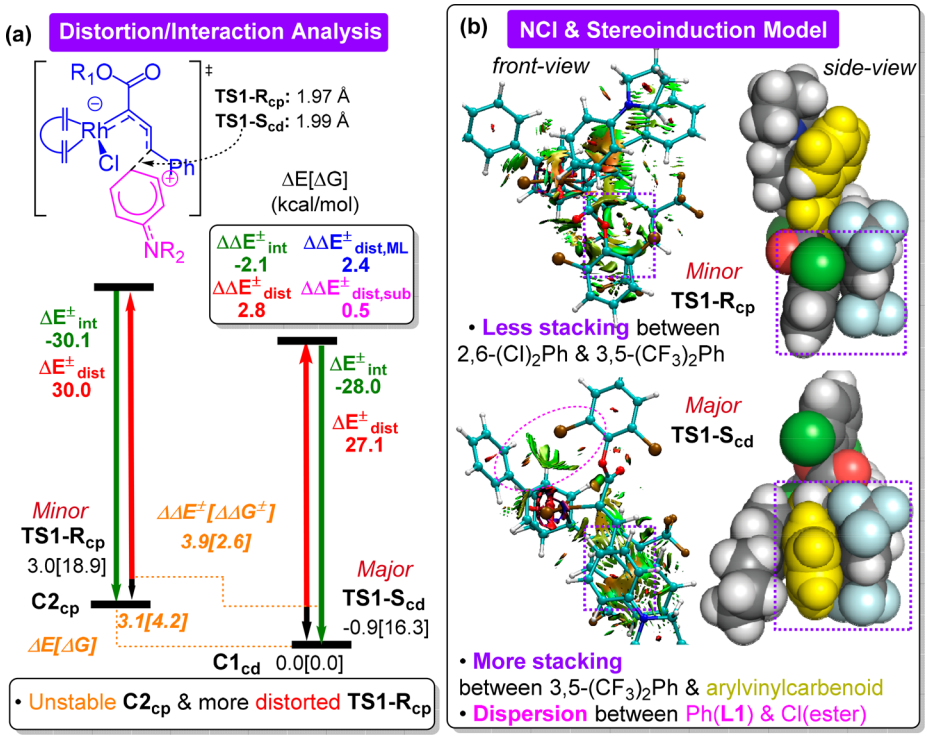

Figure 6. (a) Distortion/interaction analysis of the two key transition states by the SMD B3LYP-D3 method. (b) Noncovalent interaction (NCI) analysis (red, strong repulsion; green, weak attraction; blue, strong attraction) and stereoinduction mode of the two key transition states (side-view structures shown by the VDW representation).

https://dx.doi.org/10.1021/jacs.0c13191
J. Am. Chem. Soc. 2021, 143, 2608−2619

Scheme 8. Calculated Free Energy of the Key Steps for the (a) s-cis and (b) s-trans Rh(I) Intermediates by the SMD B3LYP-D3 Method and (c) Proposed Key Change for the Rh_2(II,II) Dimer Intermediate

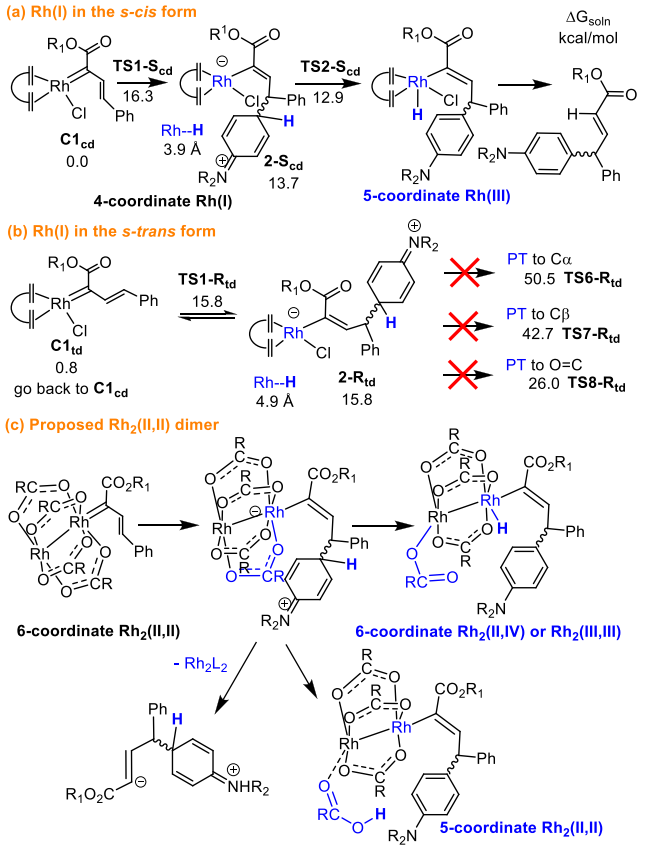

Scheme 9. Key Computational Results for the Initial Addition Step of Substrate 2u by the SMD B3LYP-D3 Method

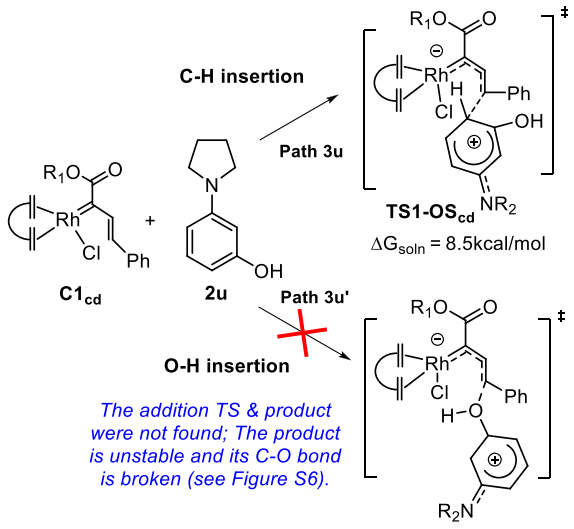

Furthermore, when the aryl group of the arylvinylcarbenoid part is swapped to have $\pi-\pi$ stacking with the C_6H_5 part of the **L1** ligand and have interactions of the chloro group (ester) with the 3,5-$(CF_3)_2$Ph group, such an isomeric addition transition state **TS1-S′$_{cd}$** ($\Delta G^{\ddagger}$ = 20.7 kcal/mol, Figure 4) becomes more unstable than **TS1-S$_{cd}$** by 4.4 kcal/mol.[18] Overall, these computational results suggest that the high stability of the **C1**-type active species and the interactions between the chiral ligand and substrates should mainly determine the observed enantioselectivity: attraction-controlled enantioselectivity.[24]

Finally, although the γ-addition in the s-trans form via **TS1-R$_{td}$** can take place with a low barrier (15.8 kcal/mol, Scheme 8b), it is impossible for subsequent zwitterionic intermediate **2-R$_{td}$** to directly transfer the proton to the Rh(I) metal due to a long separation in the *trans* configuration of **2-R$_{td}$** (H−Rh: 4.9 Å). Also, it is much more challenging for **2-R$_{td}$** to transfer the proton to the nearby carbon sites (Cα or Cβ) or carbonyl oxygen of the ester due to their much higher reaction barriers (~26.0−50.5 kcal/mol, Scheme 8b). Therefore, the γ-addition in the *s-trans* form is not the productive pathway in this present system and has to undergo the reversible process to regenerate the stable *s-cis* **C1**-type active species and aniline substrate before the productive addition pathway (e.g., Scheme 8a and Figure 5). These computational results highlight the importance of the low-valence four-coordinate Rh(I) metal to transiently donate two electrons to accept the proton and form a neutral five-coordinate Rh(III)-hydride intermediate in the current *s-cis* Rh(I)-vinylcarbenoid system. For Rh_2(II,II) dimer systems, the proton transfer from the related zwitterionic intermediate is envisioned to be energetically less favorable than our Rh(I) system, as one bridging acetate-type ligand should dissociate from one higher-valence and coordinately saturated Rh(II) metal center during two possible proton transfer processes (Scheme 8c). Alternatively, Davies, Hu, and Zhou reported that the Rh_2(II,II) zwitterionic intermediate can undergo dissociation to give a metal-free zwitterion.[4,25]

Moreover, our DFT calculations were further performed to examine the high chemoselectivity toward the C−H insertion of substrate **2u** instead of the corresponding O−H insertion (Scheme 9). The initial C−C addition step leading to the C−H insertion product was found to require a barrier of 8.5 kcal/mol via **TS1-OS$_{cd}$**. Interestingly, many attempts to locate the related C−O addition transition state and product for the O−H insertion pathway failed. The assumed C−O addition product which was found to be higher in electronic energy than **TS1-OS$_{cd}$** by about 7.5 kcal/mol can exist only when the C−O bond is fixed (Figure S6). However, the C−O bond is broken to regenerate the substrate when the C−O bond is relaxed. These computational results support the observed chemoselectivity for this Rh(I) catalyst. Furthermore, a large inverse KIE (~0.83) for more reactive substrate **2u** was also found in our SMD B3LYP-D3 study, which is comparable to that for the related 1-(3-methoxyphenyl)pyrrolidine substrate (~0.848, Scheme 5c).

CONCLUSIONS

We have developed the first example of the regiospecific and direct enantioselective C(sp^2)-H functionalization of aniline derivatives with arylvinyldiazoacetates enabled by Rh(I)-diene catalysts. A promising finding is that our chiral rhodium(I)-diene catalysts exhibit superior performance in controlling the vinylogous reactivity of arylvinylcarbenoids and achieving enantioselective variants of this chemistry. The reaction proceeds in high yield, with broad functional group compatibility, allowing access to a variety of chiral γ,γ-gem-diarylsubstituted α,β-unsaturated esters with excellent enantio-

https://dx.doi.org/10.1021/jacs.0c13191
J. Am. Chem. Soc. 2021, 143, 2608−2619

selectivities under simple and mild conditions. Moreover, such a direct enantioselective C−H functionalization reaction can also be applied to a substrate bearing an unprotected hydroxyl functionality for the first time, showing high chemoselectivity toward C−H insertion. Of particular note, the products can be transformed to a diverse set of important chiral compounds which should find applications in organic synthesis and pharmaceutical research. A combined experimental and systematic DFT study was also carried out to understand the reaction mechanism and origin of the uncommon enantio- and regioselectivity of the present Rh(I)-catalyzed insertion reaction. The observed and computed inverse deuterium KIE reflects the C−C bond formation step as the rate-determining step. Attractive interactions between the chiral ligand and substrates were also suggested to determine the enantioselectivity. Further investigations on chiral Rh(I)-carbene chemistry are ongoing in our laboratory.

■ ASSOCIATED CONTENT

Supporting Information

The Supporting Information is available free of charge at https://pubs.acs.org/doi/10.1021/jacs.0c13191.

Experimental procedures and spectroscopic data of all new compounds as well as computational details (PDF)

Accession Codes

CCDC 1978705 and 2058172 contain the supplementary crystallographic data for this paper. These data can be obtained free of charge via www.ccdc.cam.ac.uk/data_request/cif, or by emailing data_request@ccdc.cam.ac.uk, or by contacting The Cambridge Crystallographic Data Centre, 12 Union Road, Cambridge CB2 1EZ, UK; fax: +44 1223 336033.

■ AUTHOR INFORMATION

Corresponding Authors

Ming-Hua Xu − *Shenzhen Grubbs Institute and Department of Chemistry, Guangdong Provincial Key Laboratory of Catalysis, Southern University of Science and Technology, Shenzhen 518055, China; State Key Laboratory of Drug Research, Shanghai Institute of Materia Medica, Chinese Academy of Sciences, Shanghai 201203, China;* orcid.org/0000-0002-1692-2718; Email: xumh@sustech.edu.cn

Lung Wa Chung − *Shenzhen Grubbs Institute and Department of Chemistry, Guangdong Provincial Key Laboratory of Catalysis, Southern University of Science and Technology, Shenzhen 518055, China;* orcid.org/0000-0001-9460-7812; Email: oscarchung@sustech.edu.cn

Authors

Dong-Xing Zhu − *State Key Laboratory of Drug Research, Shanghai Institute of Materia Medica, Chinese Academy of Sciences, Shanghai 201203, China*

Hui Xia − *Shenzhen Grubbs Institute and Department of Chemistry, Guangdong Provincial Key Laboratory of Catalysis, Southern University of Science and Technology, Shenzhen 518055, China*

Jian-Guo Liu − *Shenzhen Grubbs Institute and Department of Chemistry, Guangdong Provincial Key Laboratory of Catalysis, Southern University of Science and Technology, Shenzhen 518055, China*

Complete contact information is available at: https://pubs.acs.org/10.1021/jacs.0c13191

Author Contributions

§D.-X.Z. and H.X. contributed equally to this work.

Notes

The authors declare no competing financial interest.

■ ACKNOWLEDGMENTS

We thank the National Science & Technology Major Project "Key New Drug Creation and Manufacturing Program", China (2018ZX09711002-006 for M.-H.X.), the National Natural Science Foundation of China (21672229, 21971103, and 81521005 for M.-H.X.; 21933003 for L.W.C.), and Guangdong Provincial Key Laboratory of Catalysis (2020B121201002 for M.-H.X. and L.W.C.) for financial support. We are especially grateful to Dr. Stefan Abele at Idorsia Pharmaceuticals Ltd., Switzerland for his very generous donation of the key intermediate (1*R*,4*R*)-5-phenylbicyclo[2.2.2]oct-5-en-2-one for diene preparation. This article is dedicated to the 10th anniversary of Chemistry Department, Southern University of Science and Technology.

■ REFERENCES

(1) (a) Davies, H. M. L.; Beckwith, R. E. J. Catalytic enantioselective C−H activation by means of metal−carbenoid-induced C−H insertion. *Chem. Rev.* **2003**, *103*, 2861. (b) Díaz-Requejo, M. M.; Pérez, P. J. Coinage metal catalyzed C−H bond functionalization of hydrocarbons. *Chem. Rev.* **2008**, *108*, 3379. (c) Doyle, M. P.; Duffy, R.; Ratnikov, M.; Zhou, L. Catalytic carbene insertion into C−H bonds. *Chem. Rev.* **2010**, *110*, 704. (d) Davies, H. M. L.; Morton, D. Guiding principles for site selective and stereoselective intermolecular C−H functionalization by donor/acceptor rhodium carbenes. *Chem. Soc. Rev.* **2011**, *40*, 1857. (e) Louillat, M.-L.; Patureau, F. W. Oxidative C−H amination reactions. *Chem. Soc. Rev.* **2014**, *43*, 901. (f) Davies, H. M. L.; Manning, J. R. Catalytic C−H functionalization by metal carbenoid and nitrenoid insertion. *Nature* **2008**, *451*, 417. (g) Ford, A.; Miel, H.; Ring, A.; Slattery, C. N.; Maguire, A. R.; McKervey, M. A. Modern Organic Synthesis with α-Diazocarbonyl Compounds. *Chem. Rev.* **2015**, *115*, 9981. (h) Che, C. M.; Lo, V. K.; Zhou, C. Y.; Huang, J. S. Selective functionalisation of saturated C-H bonds with metalloporphyrin catalysts. *Chem. Soc. Rev.* **2011**, *40*, 1950.

(2) (a) Liao, K.; Negretti, S.; Musaev, D. G.; Bacsa, J.; Davies, H. M. L. Site-selective and stereoselective functionalization of unactivated C−H bonds. *Nature* **2016**, *533*, 230. (b) Liao, K.; Pickel, T. C.; Boyarskikh, V.; Becsa, J.; Musav, D. G.; Davies, H. M. L. Site-selective and stereoselective functionalization of non-activated tertiary C−H bonds. *Nature* **2017**, *551*, 609. (c) Liao, K.; Yang, Y.-F.; Li, Y.-Z.; Sanders, J. N.; Houk, K. N.; Musaev, D. G.; Davies, H. M. L. Design of catalysts for site-selective and enantioselective functionalization of non-activated primary C−H bonds. *Nat. Chem.* **2018**, *10*, 1048.

(3) For a recent review, see (a) Li, Y.-P.; Li, Z.-Q.; Zhu, S.-F. Recent advances in transition-metal-catalyzed asymmetric reactions of diazo compounds with electron-rich (hetero-) arenes. *Tetrahedron Lett.* **2018**, *59*, 2307. For Rh(II)-catalyzed reactions, see (b) Lian, H.; Davies, H. L. M. Rhodium-catalyzed [3 + 2] annulation of indoles. *J. Am. Chem. Soc.* **2010**, *132*, 440. (c) DeAngelis, A.; Shurtleff, V. W.; Dmitrenko, O.; Fox, J. M. Rhodium(II)-catalyzed enantioselective C−H functionalization of indoles. *J. Am. Chem. Soc.* **2011**, *133*, 1650. (d) Goto, T.; Natori, Y.; Takeda, K.; Nambu, H.; Hashimoto, S. Catalytic enantioselective C−H functionalization of indoles with α-diazopropionates using chiral dirhodium(II) carboxylates: asymmetric synthesis of the (+)-α-methyl-3-indolylacetic acid fragment of acremoauxin A. *Tetrahedron: Asymmetry* **2011**, *22*, 907. For a Fe(II)-catalyzed reaction, see (e) Cai, Y.; Zhu, S.-F.; Wang, G.-P.; Zhou, Q.-L. Iron-catalyzed C-H fuctionalization of indoles. *Adv. Synth. Catal.* **2011**, *353*, 2939. For Pd(II)-catalyzed reactions, see (f) Gao, X.; Wu, B.; Huang, W.-X.; Chen, M.-W.; Zhou, Y.-G. Enantioselective palladium-catalyzed C-H functionalization of indoles

using an Axially Chiral 2,2'-bipyridine ligand. *Angew. Chem., Int. Ed.* **2015**, *54*, 11956. (g) Shen, H.-Q.; Liu, C.; Zhou, J.; Zhou, Y.-G. Enantioselective palladium-catalyzed C-H functionalization of pyrroles using an axially chiral 2,2'-bipyridine ligand. *Org. Chem. Front.* **2018**, *5*, 611. For a Cu(I)-catalyzed reaction, see (h) Gao, X.; Wu, B.; Yan, Z.; Zhou, Y.-G. Copper-catalyzed enantioselective C−H functionalization of indoles with an axially chiral bipyridine ligand. *Org. Biomol. Chem.* **2016**, *14*, 8237.

(4) Xu, B.; Li, M.-L.; Zuo, X.-D.; Zhu, S.-F.; Zhou, Q.-L. Catalytic asymmetric arylation of α-aryl-α-diazoacetates with aniline derivatives. *J. Am. Chem. Soc.* **2015**, *137*, 8700.

(5) Ma, X.-C.; Jiang, J.; Lv, S.; Yao, W.-F.; Yang, Y.; Liu, S.-Y.; Xia, F.; Hu, W. An ylide transformation of rhodium(I) carbene: enantioselective three-component reaction through trapping of rhodium(I)-associated ammonium ylides by β-nitroacrylates. *Angew. Chem., Int. Ed.* **2014**, *53*, 13136.

(6) (a) Cao, Z.; Zhao, Y.; Zhou, J. Sequential Au(I)/chiral tertiary amine catalysis: a tandem C−H functionalization of anisoles or a thiophene/asymmetric Michael addition sequence to quaternary oxindoles. *Chem. Commun.* **2016**, *52*, 2537. (b) Yu, Z.; Qiu, H.; Liu, L.; Zhang, J. Gold-catalyzed construction of two adjacent quaternary stereocenters via sequential C−H functionalization and aldol annulation. *Chem. Commun.* **2016**, *52*, 2257. (c) Ma, B.; Wu, Z.; Huang, B.; Liu, L.; Zhang, J. Gold-catalysed facile access to indene scaffolds via sequential C−H functionalization and 5-endo-dig carbocyclization. *Chem. Commun.* **2016**, *52*, 9351.

(7) (a) Davies, H. L. M.; Saikali, E.; Clark, T. J.; Chee, E. H. Anomalous reactivity of mono substituted rhodium stabilized vinylcarbenoids. *Tetrahedron Lett.* **1990**, *31*, 6299. (b) Davies, H. L. M.; Hu, B.; Saikali, E.; Bruzinski, P. R. Carbenoid versus vinylogous reactivity in rhodium(II)-stabilized vinylcarbenoids. *J. Org. Chem.* **1994**, *59*, 4535. (c) Davies, H. L. M.; Yokota, Y. Regiochemistry of molybdenum-catalyzed O−H insertions of vinylcarbenoids. *Tetrahedron Lett.* **2000**, *41*, 4851. (d) Sevryugina, Y. S.; Weaver, B.; Hansen, J.; Thompson, J.; Davies, H. L. M.; Petrukhina, M. A. Influence of electron-deficient Ruthenium(I) carbonyl carboxylates on the vinylogous reactivity of metal carbenoids. *Organometallics* **2008**, *27*, 1750. (e) Hansen, J. H.; Davies, H. L. M. Vinylogous reactivity of silver(I) vinylcarbenoids. *Chem. Sci.* **2011**, *2*, 457.

(8) (a) Yue, Y.-L.; Wang, Y.-H.; Hu, W. Regioselectivity in Lewis acids catalyzed X−H (O, S, N) insertions of methyl styryldiazoacetate with benzyl alcohol, benzyl thiol, and aniline. *Tetrahedron Lett.* **2007**, *48*, 3975. (b) Lian, Y.-J.; Davies, H. L. M. Rhodium carbenoid approach for introduction of 4-substituted (*Z*)-pent-2-enoates into sterically encumbered pyrroles and indoles. *Org. Lett.* **2010**, *12*, 924. (c) Lian, Y.-J.; Davies, H. L. M. Rh_2(*S*-biTISP)$_2$-catalyzed asymmetric functionalization of indoles and pyrroles with vinylcarbenoids. *Org. Lett.* **2012**, *14*, 1934. (d) Qin, C.; Davies, H. L. M. *Org. Lett.* **2013**, *15*, 6152. (e) Zha, G.-F.; Han, J.-B.; Hu, X.-Q.; Qin, H.-L.; Fang, W.-Y.; Zhang, C.-P. Silver-mediated direct trifluoromethoxylation of α-diazo esters via the -OCF3 anion. *Chem. Commun.* **2016**, *52*, 7458. (f) Xu, G.-Y.; Liu, K.; Dai, Z.-Y.; Sun, J.-T. Copper-catalyzed enantioselective C−H functionalization of indoles with an axially chiral bipyridine ligand. *Org. Biomol. Chem.* **2017**, *15*, 2345. (g) Ueda, J.; Harada, S.; Nakayama, H.; Nemoto, T. Silver-catalyzed regioselective hydroamination of alkenyl diazoacetates to synthesize γ-amino acid equivalents. *Org. Biomol. Chem.* **2018**, *16*, 4675.

(9) (a) Davies, H. M. L.; Stafford, D. G.; Hansen, T. Catalytic asymmetric synthesis of diarylacetates and 4,4-diarylbutanoates. a formal asymmetric synthesis of (+)-sertraline. *Org. Lett.* **1999**, *1*, 233. (b) Davies, H. M. L.; Jin, Q. Highly diastereoselective and enantioselective C−H functionalization of 1,2-dihydronaphthalenes: a combined C−H activation/Cope rearrangement followed by a retro-Cope rearrangement. *J. Am. Chem. Soc.* **2004**, *126*, 10862. (c) Davies, H. M. L.; Manning, J. R. C−H Activation as a strategic reaction: enantioselective synthesis of 4-substituted indoles. *J. Am. Chem. Soc.* **2006**, *128*, 1060. (d) Lian, Y.; Davies, H. M. L. Combined C−H functionalization/Cope rearrangement with vinyl ethers as a surrogate for the vinylogous Mukaiyama Aldol reaction. *J. Am. Chem. Soc.* **2011**, *133*, 11940.

(10) Davies and co-workers have described an interesting asymmetric example of vinylogous alkylation between methyl (*E*)-vinyldiazoacetate and *N*-heterocycles, with Rh_2(*S*-biTISP)$_2$ as catalyst, and asymmetric vinylogous selectivity was achieved to give major (*Z*)-products with good enantioselectivities (82−95% ee). See ref 8c.

(11) For reviews on chiral dienes, see (a) Johnson, J. B.; Rovis, T. More than bystanders: the effect of olefins on transition-metal-catalyzed cross-coupling reactions. *Angew. Chem., Int. Ed.* **2008**, *47*, 840. (b) Shintani, R.; Hayashi, T. Chiral diene ligands for asymmetric catalysis. *Aldrichim. Acta* **2009**, *42*, 39. (c) Feng, C.-G.; Xu, M.-H.; Lin, G.-Q. Development of bicyclo[3.3.0]octadiene- or dicyclopentadiene-based chiral diene ligands for transition-metal-catalyzed reactions. *Synlett* **2011**, *2011*, 1345. (d) Nagamoto, M.; Nishimura, T. Asymmetric transformations under iridium/chiral diene catalysis. *ACS Catal.* **2017**, *7*, 833.

(12) (a) Chen, D.; Zhang, X.; Qi, W.-Y.; Xu, B.; Xu, M.-H. Rhodium(I)-catalyzed asymmetric carbene insertion into B−H bonds: highly enantioselective access to functionalized organoboranes. *J. Am. Chem. Soc.* **2015**, *137*, 5268. (b) Chen, D.; Zhu, D.-X.; Xu, M.-H. Rhodium(I)-catalyzed highly enantioselective insertion of carbenoid into Si−H: efficient access to functional chiral silanes. *J. Am. Chem. Soc.* **2016**, *138*, 1498.

(13) (a) Yu, Z.; Ma, B.; Chen, M.; Wu, H.-H.; Liu, L.; Zhang, J. Highly site-selective direct C−H bond functionalization of phenols with α-aryl-α-diazoacetates and diazooxindoles via gold catalysis. *J. Am. Chem. Soc.* **2014**, *136*, 6904. (b) Xi, Y.; Su, Y.; Yu, Z.; Dong, B.; McClain, E. J.; Lan, Y.; Shi, X. *Angew. Chem., Int. Ed.* **2014**, *53*, 9817. (c) Zhai, C.; Xing, D.; Jing, C.; Zhou, J.; Wang, C.; Wang, D.; Hu, W. Facile synthesis of 3-aryloxindoles via Brønsted acid catalyzed Friedel−Crafts alkylation of electron-rich arenes with 3-diazooxindoles. *Org. Lett.* **2014**, *16*, 2934. (d) Yu, Z.; Li, Y.; Shi, J.; Ma, B.; Liu, L.; Zhang, J. $(C_6F_5)_3B$ Catalyzed chemoselective and *ortho*-selective substitution of phenols with α-aryl α-diazoesters. *Angew. Chem., Int. Ed.* **2016**, *55*, 14807. (e) Yu, Z.; Li, Y.; Zhang, P.; Liu, L.; Zhang, J. Ligand and counteranion enabled regiodivergent C−H bond functionalization of naphthols with α-aryl-α-diazoesters. *Chem. Sci.* **2019**, *10*, 6553.

(14) Denton, J. R.; Davies, H. M. L. Enantioselective reactions of donor/acceptor carbenoids derived from α-aryl-α-diazoketones. *Org. Lett.* **2009**, *11*, 787.

(15) CDCC 1978705. See the SI for details.

(16) For selected examples of biologically active compounds containing 2,3-dihydrobenzofurans, see (a) Cao, Y.-G.; Zheng, X.-K.; Yang, F.-F.; Li, F.; Qi, M.; Zhang, Y.-L.; Zhao, X.; Kuang, H.-X.; Feng, W.-S. Two new phenolic constituents from the root bark of Morus alba L. and their cardioprotective activity. *Nat. Prod. Res.* **2018**, *32*, 391. (b) Surapinit, S.; Sri-in, P.; Tip-pyang, S. Highly potent oligostilbene sbLOX-1 inhibitor from gnetum macrostachyum. *Nat. Prod. Commun.* **2014**, *97*, 969.

(17) Selected computational studies on reactions of transition-metal carbene with σ-bonds: (a) Liang, Y.; Zhou, H.; Yu, Z. X. Why is copper(I) complex more competent than dirhodium(II) complex in catalytic asymmetric O-H insertion reactions? A computational study of the metal carbenoid O-H insertion into water. *J. Am. Chem. Soc.* **2009**, *131*, 17783. (b) Hansen, J. H.; Gregg, T. M.; Ovalles, S. R.; Lian, Y.; Autschbach, J.; Davies, H. M. L. On the Mechanism and Selectivity of the Combined C−H Activation/Cope Rearrangement. *J. Am. Chem. Soc.* **2011**, *133*, 5076. (c) Liu, Y.; Yu, Z.; Zhang, J. Z.; Liu, L.; Xia, F.; Zhang, J. Origins of unique gold-catalysed chemo- and site-selective C−H functionalization of phenols with diazo compounds. *Chem. Sci.* **2016**, *7*, 1988. (d) Nakamura, E.; Yoshikai, N.; Yamanaka, M. Mechanism of C−H Bond Activation/C−C Bond Formation Reaction between Diazo Compound and Alkane Catalyzed by Dirhodium Tetracarboxylate. *J. Am. Chem. Soc.* **2002**, *124*, 7181. (e) Hare, S. R.; Tantillo, D. J. Cryptic post-transition state bifurcations that reduce the efficiency of lactone-forming Rh-carbenoid C−H insertions. *Chem. Sci.* **2017**, *8*, 1442. (f) Song, L.;

https://dx.doi.org/10.1021/jacs.0c13191
J. Am. Chem. Soc. 2021, 143, 2608−2619

Feng, Q.; Wang, Y.; Ding, S.; Wu, Y.-D.; Zhang, X.; Chung, L. W.; Sun, J. Ru-Catalyzed Migratory Geminal Semihydrogenation of Internal Alkynes to Terminal Olefins. *J. Am. Chem. Soc.* **2019**, *141*, 17441. (g) Yang, L. L.; Evans, D.; Xu, B.; Li, W. T.; Li, M. L.; Zhu, S. F.; Houk, K. N.; Zhou, Q. L. Enantioselective Diarylcarbene Insertion into Si-H Bonds Induced by Electronic Properties of the Carbenes. *J. Am. Chem. Soc.* **2020**, *142*, 12394. (h) Liu, S.; Jiang, J.; Chen, J.; Wei, Q.; Yao, W.; Xia, F.; Hu, W. A DFT calculation-inspired Rh(I)-catalyzed reaction via suppression of α-H shift in α-alkyldiazoacetates. *Chem. Sci.* **2017**, *8*, 4312. (i) Weldy, N. M.; Schafer, A. G.; Owens, C. P.; Herting, C. J.; Varela-Alvarez, A.; Chen, S.; Niemeyer, Z.; Musaev, D. G.; Sigman, M. S.; Davies, H.; Blakey, S. B. Iridium(iii)-bis(imidazolinyl)phenyl catalysts for enantioselective C-H functionalization with ethyl diazoacetate. *Chem. Sci.* **2016**, *7*, 3142. (j) Besora, M.; Olmos, A.; Gava, R.; Noverges, B.; Asensio, G.; Caballero, A.; Maseras, F.; Pérez, P. J. A Quantitative Model for Alkane Nucleophilicity Based on C-H Bond Structural/Topological Descriptors. *Angew. Chem., Int. Ed.* **2020**, *59*, 3112.

(18) When the aryl group of the arylvinylcarbenoid part of $\mathbf{C1}_{cd}$ is switched to stack with an unfunctionalized C_6H_5 part of the **L1** ligand in another closed quadrant of the catalyst, such that conformer ($\mathbf{C1'}_{cd}$) is computed to become unstable by 2.9 kcal/mol (Table S1). Our energy decomposition analysis (EDA) showed that larger interactions (particularly the charge-transfer part) between the (**L1**) Rh and arylvinylcarbene parts were found in $\mathbf{C1}_{cd}$ than in $\mathbf{C1'}_{cd}$ (Table S3 and Figure S1).

(19) (a) Alternatively, the γ-addition can proceed through another competitive isomeric transition state $\mathbf{TS1\text{-}S}_{cp}$ with a slightly higher barrier (16.5 kcal/mol; Figure 4). The major geometric difference between $\mathbf{TS1\text{-}S}_{cp}$ and $\mathbf{TS1\text{-}S}_{cd}$ is a rotation of the ester group. (b) Other conformations for the γ-addition and α-addition transition states were also searched and found to be high in energy (Figure S2 and Table S5). (c) The key mechanistic conclusion is qualitatively supported by the DLPNO-CCSD(T0)//SMD B3LYP-D3, SMD PBE0-D3//SMD B3LYP-D3, and SMD ωB97XD//SMD B3LYP-D3 methods (Tables S8 and S9).

(20) $\mathbf{TS2\text{-}S}_{cd}$ is higher in electronic energy than $\mathbf{3}_{cd}$ by 1.6 kcal/mol in solution but becomes lower in energy than $\mathbf{3}_{cd}$ when including the effect of the zero-point energy correction (Table S5).

(21) (a) Anslyn, E. V.; Dougherty, D. A. *Modern Physical Organic Chemistry*; University Science Books, 2006. (b) Yang, Y.; Zhang, X.; Zhong, L.-P.; Lan, J.; Li, X.; Li, C.-C.; Chung, L. W. Unusual KIE and dynamics effects in the Fe-catalyzed hetero-Diels-Alder reaction of unactivated aldehydes and dienes. *Nat. Commun.* **2020**, *11*, 1850. (c) Van Sickle, D. E.; Rodin, J. O. The secondary deuterium isotope effect on the Diels-Alder reaction. *J. Am. Chem. Soc.* **1964**, *86*, 3091. (d) The more reactive substrate should have an earlier transition state with a longer C−C bond-forming distance and a larger KIE value, based on Hammond's postulate. (e) Ford, D. D.; Lehnherr, D.; Kennedy, C. R.; Jacobsen, E. N. On- and Off-Cycle Catalyst Cooperativity in Anion-Binding Catalysis. *J. Am. Chem. Soc.* **2016**, *138*, 7860. (f) Wolf, J. R.; Hamaker, C. G.; Djukic, J.-P.; Kodadek, T.; Woo, L. K. Shape and stereoselective cyclopropanation of alkenes catalyzed by iron porphyrins. *J. Am. Chem. Soc.* **1995**, *117*, 9194.

(22) (a) Morokuma, K. Why do molecules interact? The origin of electron donor-acceptor complexes, hydrogen bonding and proton affinity. *Acc. Chem. Res.* **1977**, *10*, 294. (b) Nagase, S.; Morokuma, K. An ab initio molecular orbital study of organic reactions. The energy, charge, and spin decomposition analyses at the transition state and along the reaction pathway. *J. Am. Chem. Soc.* **1978**, *100*, 1666. (c) Ess, D. H.; Houk, K. N. Distortion/Interaction Energy Control of 1,3-Dipolar Cycloaddition Reactivity. *J. Am. Chem. Soc.* **2007**, *129*, 10646. (d) Lan, J.; Liao, T.; Zhang, T.; Chung, L. W. Reaction Mechanism of Cu(I)-Mediated Reductive CO2 Coupling for the Selective Formation of Oxalate: Cooperative CO2 Reduction To Give Mixed-Valence Cu2(CO2•-) and Nucleophilic-Like Attack. *Inorg. Chem.* **2017**, *56*, 6809. (e) Chen, C.; Zhang, Z.; Jin, S.; Fan, X.; Geng, M.; Zhou, Y.; Wen, S.; Wang, X.; Chung, L. W.; Dong, X. Q.; Zhang, X. Enzyme-Inspired Chiral Secondary-Phosphine-Oxide Ligand with Dual Noncovalent Interactions for Asymmetric Hydrogenation. *Angew. Chem., Int. Ed.* **2017**, *56*, 6808. (f) Fernández, I.; Bickelhaupt, F. M. The activation strain model and molecular orbital theory: understanding and designing chemical reactions. *Chem. Soc. Rev.* **2014**, *43*, 4953. (g) Bickelhaupt, F. M.; Houk, K. N. Analyzing Reaction Rates with the Distortion/Interaction-Activation Strain Model. *Angew. Chem., Int. Ed.* **2017**, *56*, 10070.

(23) Johnson, E. R.; Keinan, S.; Mori-Sánchez, P.; Contreras-García, J.; Cohen, A. J.; Yang, W. Revealing Noncovalent Interactions. *J. Am. Chem. Soc.* **2010**, *132*, 6498.

(24) (a) Liu, J.; Nie, M.; Zhou, Q.; Chung, L. W.; Tang, W.; Ding, K. Enantioselective palladium-catalyzed diboration of 1,1-disubstituted allenes. *Chem. Sci.* **2017**, *8*, 5161. (b) Lu, G.; Liu, R. Y.; Yang, Y.; Fang, C.; Lambrecht, D. S.; Buchwald, S. L.; Liu, P. Ligand-Substrate Dispersion Facilitates the Copper-Catalyzed Hydroamination of Unactivated Olefins. *J. Am. Chem. Soc.* **2017**, *139*, 16548. (c) Wang, T.; Zhuo, L.-G.; Li, Z.; Chen, F.; Ding, Z.; He, Y.; Fan, Q.-H.; Xiang, J.; Yu, Z.-X.; Chan, A. S. C. Highly Enantioselective Hydrogenation of Quinolines Using Phosphine-Free Chiral Cationic Ruthenium Catalysts. Scope, Mechanism, and Origin of Enantioselectivity. *J. Am. Chem. Soc.* **2011**, *133*, 9878.

(25) (a) Jia, S.; Xing, D.; Zhang, D.; Hu, W. Catalytic Asymmetric Functionalization of Aromatic C−H Bonds by Electrophilic Trapping of Metal-Carbene-Induced Zwitterionic Intermediates. *Angew. Chem., Int. Ed.* **2014**, *53*, 13098. (b) Guo, X.; Hu, W. Novel Multicomponent Reactions via Trapping of Protic Onium Ylides with Electrophiles. *Acc. Chem. Res.* **2013**, *46*, 2427. (c) Davies, H. M. L.; Jin, Q. Double C−H Activation Strategy for the Asymmetric Synthesis of C2-Symmetric Anilines. *Org. Lett.* **2004**, *6*, 1769. (d) Schmid, S. C.; Guzei, I. A.; Fernández, I.; Schomaker, J. M. Ring Expansion of Bicyclic Methyleneaziridines via Concerted, Near-Barrierless [2,3]-Stevens Rearrangements of Aziridinium Ylides. *ACS Catal.* **2018**, *8*, 7907−7914. (e) Eshon, J.; Nicastri, K. A.; Schmid, S. C.; Raskopf, W. T.; Guzei, I. A.; Fernández, I.; Schomaker, J. M. Intermolecular [3 + 3] ring expansion of aziridines to dehydropiperi-dines through the intermediacy of aziridinium ylides. *Nat. Commun.* **2020**, *11*, 1273 and ref 4.

https://dx.doi.org/10.1021/jacs.0c13191
J. Am. Chem. Soc. 2021, 143, 2608−2619